

Running title: TRANS-BERINGIA DISPERSALS OF BARKLICE

**Multiple trans-Beringia dispersals of the barklouse genus  
*Trichadenotecnum* (Insecta: Psocodea: Psocidae)**

KAZUNORI YOSHIKAWA 1\*, KEVIN P. JOHNSON 2, IZUMI YAO 1, JOSÉ ARTURO  
CASASOLA GONZÁLEZ 3, EMILIE BESS 2,4 and ALFONSO NERI GARCÍA  
ALDRETE 5

1 *Systematic Entomology, School of Agriculture, Hokkaido University, 060-8589, Japan*

2 *Illinois Natural History Survey, University of Illinois, Champaign, IL 61820, USA*

3 *Instituto de Estudios Ambientales, Universidad de la Sierra Juárez, 68725 Oaxaca, Mexico*

4 *The Evergreen State College, Olympia, Seattle, WA 98505, USA*

5 *Instituto de Biología, Departamento de Zoología, UNAM, CdMx, México, 04510, Mexico*

\*Corresponding author.

E-mail: [psocid@res.agr.hokudai.ac.jp](mailto:psocid@res.agr.hokudai.ac.jp)

## Abstract

The causes underlying disjunct distributions are of major importance in biogeography. Arcto-Tertiary relict biotas in the temperate northern hemisphere, which typically show disjunct distributions between Asia and the Nearctic region, are widely known but often poorly understood examples of disjunct distributions. The distributional pattern of the barklouse genus *Trichadenotecnum* is an example of an Arcto-Tertiary relict, with centers of species diversity in Asia and Central America. We evaluated the potential causes of this disjunct distribution in *Trichadenotecnum* using a molecular phylogeny, divergence dating, and ancestral area reconstruction. Phylogenetic analysis identified three separate clades of New World *Trichadenotecnum*, whereas all other groups were distributed in the Old World. Ancestral area and dating analyses recovered three independent events of trans-Beringian dispersal in the Oligocene to Miocene (27–15 MYA). The formation of two disjunct centers of diversity can be explained by the restriction of distributional areas to temperate refugia during the Quaternary glaciations (2.5–0.02 MYA). The South American *Trichadenotecnum* appeared to have arisen from two independent dispersal events in the Miocene (19–9 MYA). These estimated dispersal dates are much older than the generally assumed date (Pleistocene: ca. 3 MYA) for the formation of the Isthmus of Panama.

**ADDITIONAL KEYWORDS:** Arcto-Tertiary relict biota – Beringia – Isthmus of Panama – molecular phylogeny – molecular dating – ancestral area reconstruction

## INTRODUCTION

Arcto-Tertiary relict animals and plants, with distributions in both the Palearctic and Nearctic regions, constitute important elements of the present biodiversity of the temperate northern hemisphere (Tiffney, 1985; Wen, 1999; Milne & Abbott, 2002). Typically, Arcto-Tertiary relict organisms show disjunct distributions between eastern Asia and the Nearctic (e.g., Milne, 2006). During the Paleogene and Neogene (ca. 66–2.6 MYA), when the climate was temperate, ancestors of Arcto-Tertiary organisms were widely distributed continuously throughout the northern hemisphere. The Bering Landbridge, or Beringia (Fig. 1), is generally considered to be the main dispersal pathway of Arcto-Tertiary organisms between Asia and the Nearctic. In the Quaternary (2.5 MYA to present), due to the radical climate cooling and glaciation, the distribution of these organisms shifted to low latitude areas, causing the present disjunct distributional patterns for taxa limited to temperate regions. This scenario for the origins of the Arcto-Tertiary biota, first constructed based on phytogeographic studies (e.g., Chaney, 1947), is widely accepted. Definitive support for this traditional view was provided recently using molecular phylogenetic and biogeographical analyses of blue butterflies (Vila *et al.*, 2011).

The North Atlantic Land Bridge (NALB: Fig. 1) is another potential gateway connecting the Palearctic and Nearctic regions. The NALB is usually thought to be less important in generating modern distributional patterns, because Arcto-Tertiary relict organisms are typically distributed in eastern Asia, not Europe (Fig. 1). In addition, the NALB is thought to have disappeared in the Paleogene (~ 30 MYA), whereas the Bering land bridge is thought to have remained until the late Neogene (~ 3 MYA). However, some recent studies have cast doubt on this traditional assumption (e.g., Sanmartín, Enghoff & Ronquist, 2001; Milne, 2006). For example, the extant species of the relict nymphomyiid flies are known only from eastern Asia and the Nearctic as is typically the case for Arcto-Tertiary relicts. However, the discovery of a fossil nymphomyiid fly species from Baltic (European) amber and its closer relatedness to the Nearctic species (Wagner, Hoffeins & Hoffeins, 2000) show the potential importance of the NALB gateway. Furthermore, new paleobotanical evidence strongly suggests that NALB may have remained as a connection much longer than previously thought, possibly up until the mid Neogene (6 MYA: Denk, Grimsson & Zetter, 2010; Denk *et al.*, 2011). Further biogeographic studies of Arcto-Tertiary relict taxa based on reliable phylogenies are needed to understand the historical backgrounds of transcontinental

disjunct distributions.

Barklice, also known as psocids or "Psocoptera", are free-living insects belonging to the order Psocodea. These small to mid-sized insects (ca. 1–10 mm in length) inhabit a wide range of habitats, such as tree trunks or twigs, stone surfaces, living or dead foliage, or leaf litter. The genus *Trichadenotecnum* (Psocidae) is one of the most species-rich genera of barklice, containing about 200 species (Lienhard & Smithers, 2002; Lienhard, 2003–2016). Members of this genus inhabit tree trunks, twigs, or stone surfaces and feed on lichens. The genus *Trichadenotecnum* has a worldwide distribution, but there are two widely disjunct areas of high species diversity: in Southeast to eastern Asia (ca. 150 species: Yoshizawa *et al.*, 2014; Yoshizawa & Lienhard, 2015a, b) and in Central America (ca. 35 species: Yoshizawa *et al.*, 2008). This disjunct pattern of diversity hotspots makes *Trichadenotecnum* an example of an Arcto-Tertiary relict taxon (Yoshizawa, García Aldrete & Mockford, 2008).

A recent morphology-based phylogenetic analysis of *Trichadenotecnum* indicated that the genus has its origin in the Old World, and three separate clades dispersed to and colonized the New World (Yoshizawa *et al.*, 2008: Fig. 1). These three clades are highly variable in their level of divergence: the oldest clade (Neotropical [NT] clade in Fig. 1) represents the deepest split of the genus, the youngest clade (*alexandrae* group in Fig. 1) constitutes a very closely related complex of species, and the intermediate clade (North-Central-South America [NCS] clade in Fig. 1) contains about 35 species. These clades are expected to have different histories of dispersal, diversification, and extinction. Thus, by focusing on *Trichadenotecnum*, the different scales of biogeographical history experienced by this Arcto-Tertiary relict taxon can be analyzed simultaneously. In addition, at least two clades of *Trichadenotecnum* have been suggested to have crossed the Isthmus of Panama to South America (Yoshizawa *et al.*, 2008; Yoshizawa, Souza-Silva & Ferreira, in press: Fig. 1). The date of the formation of the Isthmus is also a recently debated subject (Montes *et al.*, 2015; O'Dea *et al.*, 2016), for which dating the origins of South American *Trichadenotecnum* is relevant.

In the present study, we estimated the global phylogeny of the genus *Trichadenotecnum* based on five gene markers from both nuclear and mitochondrial genomes. The samples included almost all species groups recognized to date, and the sampled areas cover almost the entire distributional range of the genus. Based on the resulting phylogeny of this genus, we conducted divergence dating and biogeographical analyses to elucidate the

historical context of the present distributional pattern of *Trichadenotecnum*.

## **MATERIALS AND METHODS**

### **Phylogenetic and Divergence Time Estimation**

Samples used in this study were freshly killed and stored in 80% or 95% ethanol. Partial sequences of the nuclear *18S rRNA* and *Histone 3* and mitochondrial *16S rRNA*, *12S rRNA*, and *COI* genes were used for analyses. Methods for DNA extraction, PCR amplification, sequencing and alignment followed Yoshizawa & Johnson (2010). The aligned data set is available as Appendix S1–2. Sequences obtained from the New World *Trichadenotecnum* species (Table 1) were appended to the data matrix of the Old World *Trichadenotecnum* generated by Yoshizawa, Yao & Lienhard (2016). Most of the New World specimens were females and thus could not be identified to species. An additional newly obtained sample from the Afrotropical region (a female specimen from the United Arab Emirates) was also included. In addition, several outgroup sequences were also included to provide calibration points for the tree as follows: more distant outgroups (Hemipsocidae, Psilopsocidae, Myopsocidae, and Psocidae of the infraorder Psocetae: Yoshizawa & Johnson, 2014) as a calibration point based on the oldest fossil record of Psocidae (Engel & Perkovsky, 2006); Hawaiian *Ptycta* as a calibration point based on the previous estimation (Bess, Catanach & Johnson, 2013).

Using the aligned data set, maximum-likelihood (ML) and Bayesian analyses were conducted. We combined all datasets into a single matrix and analyzed them simultaneously (Yoshizawa & Johnson, 2008). The best fit model for the ML analysis was estimated using the hierarchical likelihood ratio test (hLRT) as implemented in jModelTest 2.1.1 (Posada, 2008). The best model was selected based on a BioNJ tree. As a result, the GTR+Gamma+Invariable site model was selected (parameters described in Appendix S1). ML tree searches were conducted using PAUP\* 4b149 (Swofford 2002). BioNJ, IQ-TREE (Nguyen *et al.*, 2015), and Bayesian trees were used as starting trees, and TBR branch swapping was conducted. The most likely tree was found when the Bayesian tree was designated as the starting tree. Ultrafast likelihood bootstrap (Minh, Nguyen & von Haeseler, 2013) was performed using IQ-TREE 1.4.3 with 1000 replicates.

We used MrBayes 3.2.1 (Ronquist & Huelsenbeck, 2003) for Bayesian analyses. Data were subdivided into nine categories (*18S*, *16S*, *12S*, and first, second, and third codon

positions of both *Histone 3* and *COI*), and the substitution models were estimated separately for each category using hLRT as implemented in MrModeltest 2.3 (Nylander 2004). Settings for Bayesian analyses are described in Appendix S1. We performed two runs each with four chains for 30 million generations and trees were sampled every 1000 generations. The first 50% of the sampled trees were excluded as burn-in, and a 50% majority consensus tree was computed to estimate posterior probabilities.

For divergence date estimation, a Bayesian method was adopted using the software MCMCtree in the PAML 4.8 software package (Yang, 2007). First, we estimated the substitution rate prior using the divergence date 7.1 MYA for the Hawaiian *Ptycta* (Bess *et al.*, 2013). Based on the result, a gamma prior for the substitution rate was set. The GTR+G model was adopted with an  $\alpha = 0.6$ , which was a close approximation of the best substitution model estimated by jModeltest. We performed a run for 100000 generations, and the values were sampled every 50 generations. The first 50% of the obtained values were excluded for burn-in. For dating analysis, two calibration points (minimum 33.9 MYA for Psocidae–Myopsocidae based on the oldest fossil species of Psocidae, *Psocidus multiplex* (Roesler, 1943); 4.7–10.05 MYA for basal divergence of *Ptycta* based on the previous estimation) were selected (Fig. 2). A fossil species of *Trichadenotecnum*, *T. trigonoscenea* (Enderlein, 1911), is known from Oligocene (34–23 MYA) but, judging from its original description and subsequent redescription (Enderlein, 1911, 1929), its assignment to *Trichadenotecnum* cannot be justified. Therefore, this record was not used for tree calibration.

In addition, we also performed a phylogenetic analysis of seven samples of the *alexanderae* group. Only the *COI* gene was used for this separate analysis for the following reasons: 1) samples from two localities (Shikoku and Tsushima) were only available as old specimens for which amplification of other genes failed; 2) all samples are nearly genetically identical and almost no variation can be found in other genes; 3) only the *COI* gene contained sufficient variation and was able to provide enough resolution with high confidence. The substitution model for this analysis was determined using jModeltest. An ML analysis with an exhaustive tree search was performed using PAUP (Appendix S2). This tree was rooted by the *alinguum* group.

## **Biogeographical Analysis**

Ancestral area reconstruction was performed using the ML tree. Non-*Trichadenotecnum* samples were excluded from the analysis. We used Dispersal-Extinction-Cladogenesis (DEC) model (from Lagrange: Ree & Smith, 2008) as implemented in the software RASP 3.2 (Yu *et al.*, 2015). Dispersal-Vicariance Analysis (DIVA: Ronquist, 1997) was a potential alternative to the DEC model. However, the primary assumption of DIVA is that vicariance provides the simplest explanation for any historical changes in biogeographical distribution and is thus not appropriate for explaining widely disjunct transcontinental distributional patterns. Seven geographical regions were defined: Afrotropical, Western Palearctic, Eastern Palearctic, Oriental, North America, Central America, and South America (Wallace, 1876). Dispersal events were permitted only between neighboring regions (see map in Fig. 4), including between the Western Palearctic and North America (via the NALB) and between the Eastern Palearctic and North America (via Beringia) (Fig. 1). The maximum number of areas allowed for ancestral distributions at each node was set to two, mirroring the current distribution of species. The biogeographical region coding of each sample was based on the known distributional range of the species. The only exception was *T. circularoides*, which is a parthenogenetic species known to have been introduced to multiple regions recently (Yoshizawa, 2004). Its bisexual sister species (*T. gonzalezi*: not sampled in the present study), and also their close relatives, are only distributed in South America (Yoshizawa *et al.*, 2008). Therefore, South America was coded for *T. circularoides*.

Ancestral area reconstruction was performed separately for the *alexanderae* group (Fig. 1). We used a likelihood-based StochChar module as implemented in Mesquite (Maddison & Maddison, 2016) for the ancestral area estimation of the *alexanderae* group because Lagrange analysis requires a fully bifurcating tree and the tree of the *alexanderae* group contained polytomies.

## RESULTS

The aligned data set consisted of 447 bp of *18S*, 327 bp of *Histone 3*, 455 bp (with four excluded characters) of *16S*, 351 bp (with five excluded characters) of *12S*, and 352 bp of *COI*. The phylogenetic analyses of the combined data provided well resolved trees. ML (Fig. 2) and Bayesian trees were highly concordant, except for the arrangement of some shallow and weakly supported branches, which do not affect the final conclusions of this

study. The tree was concordant with the phylogeny estimated for the Old World *Trichadenotecnum* (Yoshizawa *et al.*, 2016) and also relatively concordant with the morphology-based tree (Yoshizawa *et al.*, 2008).

The New World species of *Trichadenotecnum* were divided into three clades (Fig. 2), as also recovered using morphological data (Yoshizawa *et al.*, 2008). The first clade was composed of the *circularoides* + *roesleri* groups (referred to as the NT [Neotropical] clade hereafter because they are exclusively distributed in the Neotropical Region: Fig. 2), small species groups containing three and four species, respectively. The monophyly of the NT clade was strongly supported (98% bootstrap [BS] and 100% posterior probability [PP]). This clade was estimated to have diverged from other *Trichadenotecnum* around 27 million years ago (MYA: Fig. 3). Monophyly of a group comprising the remainder of *Trichadenotecnum* was fairly well supported (52% BS, 100% PP) (Fig. 2). The divergence date of two groups of the NT clade was estimated as 19 MYA (Fig. 3), and their ancestral area was estimated as Central (F) to South America (G) (Fig. 4; Appendix S3).

The second clade was composed of the *slossonae* + *chiapense* + *quaesitum* + *concinnum* + *desolatum* groups distributed in North, Central, and South America (referred to as the NCS clade: corresponding the New World bulky clade *sensu* Yoshizawa *et al.*, 2008: Fig. 2). This highly diverse clade was strongly supported as monophyletic (99% BS, 100% PP). The sister group of the NCS clade was not identified with confidence. The divergence date between the NCS clade and other lineages was estimated at 19 MYA (Fig. 3), and the basal divergence within the NCS clade was estimated at 17 MYA (Fig. 3). The ancestral area of the NCS clade was estimated to be North to Central America (EF), and that of the NCS plus its sister clade was estimated as eastern Palearctic to North America (CE) or eastern Eurasia (CD) (Fig. 4; Appendix S3). Contrary to morphological analysis (Yoshizawa *et al.*, 2008), the *slossonae* group was identified as the sister of the remaining members of the NCS clade. Monophyly of the *chiapense* + *quaesitum* + *concinnum* groups was strongly supported (100% BS, PP), and this clade was confidently placed sister to the *desolatum* group (98% BS, 100% PP) (Fig. 2).

The third clade was the *alexanderae* group from Japan and North America. This clade is composed of a species complex containing *T. alexanderae* and sibling parthenogenetic species (100% BS, PP). This clade was placed sister to the *alinguum* group with fairly strong support values (82% BS, 95% PP) (Fig. 2). The estimated divergence time between these two



groups was 15 MYA (Fig. 3), and their ancestral distributional area was most likely Eastern Palearctic (C) and/or Oriental (D) (Fig. 4; Appendix S3). The divergence date between two *alexanderae* clades was estimated at 0.9 MYA (Fig. 3), and their ancestral area was estimated as eastern Palearctic plus North America (CE) (Fig. 4).

A separate phylogenetic analysis for the *alexanderae* group identified two clades, with their uncorrected *P*-distance of the *COI* gene = 0.0171–0.0257 (Fig. 5). Both clades contained Japanese and USA samples and, in one case, the samples from the two different regions (Honshu.369 and KPJ-2003) showed an identical haplotype.

## DISCUSSION

The molecular phylogeny indicates that New World *Trichadenotecnum* form three separate clades within the genus (Figs 1–2), with the remaining taxa distributed in the Old World. Two alternative hypotheses, vicariance or dispersal, could potentially explain this transcontinental distribution. Of them, the Gondwanan vicariance hypothesis is unlikely because the origin of *Trichadenotecnum* (27 MYA) (Fig. 3) is far younger than the break-up of Gondwana (80–184 MYA). Therefore, the dispersal hypothesis, via either the North Atlantic Land Bridge (NALB) or Beringia, are likely explanations of the transcontinental distribution of *Trichadenotecnum*.

Divergence of the oldest New World clade (the NT clade) from the rest of *Trichadenotecnum* is estimated to occur in the late Paleogene (around 27 MYA). A deep divergence within this clade is estimated to have occurred in the Neogene (around 19 MYA). Divergence of the second major New World clade (the NCS clade) from its sister is estimated to have occurred in the Neogene, at 19 MYA. The Bering land bridge is generally thought to have remained connected until 3.1–4.1 MYA (Marincovich Jr & Gladenkov, 1999), so dispersal of these clades through Beringia is likely. The NALB is generally thought to have disappeared by the mid Paleogene (~30 MYA), and, if this is the case, the NALB becomes less likely as a dispersal route between Eurasia and North America. However, some recent studies have suggested that the NALB remained until the Miocene (6 MYA, Denk *et al.*, 2010, 2011) providing a possible dispersal route.

Ancestral area reconstruction suggests that eastern Eurasia (CD) or the eastern Palearctic + North America (CE) was the ancestral distributional area of the ancestor of the NCS clade + sister taxa (Fig. 4; Appendix S3). The exact sister taxon of the NCS clade is still

ambiguous (Fig. 2), and the possibility that the *kruciliense* group is sister to the NCS clade cannot be ruled out (Fig. 2). However, the eastern Palearctic + North America regions (CE) were identified as the most likely ancestral area even if the *kruciliense* group was designated to be the sister of the NCS clade (Appendix S4). Therefore, Beringia seems to be the most likely dispersal route for the ancestor of the NCS clade. The NT clade is sister to all other *Trichadenotecnum*, though the sister taxon of *Trichadenotecnum* has not been identified with confidence (Yoshizawa & Johnson, 2008; Yoshizawa *et al.*, 2016). Thus, although the eastern Palearctic + North America regions (CE) were estimated as the most likely distributional area of the common ancestor of *Trichadenotecnum*, it remains possible that including comprehensive outgroup sampling that identifies the sister taxon of *Trichadenotecnum* could change this result. In addition, the current analysis cannot identify the direction of dispersal.

The biogeographical analysis strongly suggested that the ancestors of both New World NT and NCS clades first occurred in North America (E) (Fig. 4). However, the distribution of these clades is such that they are now completely absent (NT clade) or very limited (NCS clade) in North America (Fig. 1). In addition, all the North American species of the NCS clade (*T. slossonae*, *T. quaesitum*, and *T. desolatum*) are also distributed in Mexico, suggesting their more northerly distribution is the result of a more recent event. These results suggest that *Trichadenotecnum* experienced mass extinction in North America, probably during the glaciation periods after the Miocene, including the Last Glacial Maxima (Wolfe, 1994; Zachos *et al.*, 2001; Micheels *et al.*, 2007). Judging from high diversity of the NCS clade in Central America (Yoshizawa *et al.*, 2008), this area likely acted as a refugium during the glaciation periods, and more northerly refugia (e.g., Walker *et al.*, 2009; Roberts & Hamann, 2015) were probably not suitable for the survival of *Trichadenotecnum*. Palearctic *Trichadenotecnum* also probably experienced mass extinction during periods of glaciation, because the species richness of the genus in this region (except for the Sino-Japanese region *sensu* Holt *et al.*, 2013) is low, especially in Europe. However, there are some highly diverged European species (e.g., *T. sexpunctatum* distributed in Europe including mountainous regions and *T. germanicum* distributed in Europe to Mongolia north to Finland: Fig. 3), suggesting that European refugia (e.g., Petit *et al.*, 2003) were suitable for these *Trichadenotecnum* species to survive during periods of glaciation.

As discussed above, both NT and NCS clades began diversifying in the New World during the Neogene, and the origin of the NT clade is older than that of the NCS clade.

However, the distributional range and species richness of the two clades are significantly different; species of the NCS clade are widely distributed and highly diverse in Central America, whereas the diversity of the NT clade is low and its distribution is mostly restricted to South America (Fig. 1). These differences are likely explained by their cold tolerance. In tropical regions, species of *Trichadenotecnum s.str.* (including the NCS clade: Fig. 2) are common in higher altitude areas (Yoshizawa, Lienhard & Idris, 2014; Yoshizawa & Lienhard, 2015a; Yoshizawa *et al.*, in press) but rare in lowland areas. In contrast, all species of the NT clade occur only in the lowland tropics (Yoshizawa *et al.*, 2008). It seems likely that species of the NCS clade are more tolerant of low temperature than those of the NT clade, and may have survived more readily during glacial periods in Central America.

The biogeographical analyses also suggested that both NT and NCS clades dispersed from Central to South America. The distributional range of the NCS clade in South America was thought to be restricted to the northern-most regions because of recent dispersal that followed the formation of the Isthmus of Panama (Pliocene: ca. 3 MYA) (Yoshizawa *et al.*, 2008). However, a species of the NCS clade (*T. ufla*) was discovered recently from southeastern Brazil (Yoshizawa *et al.*, in press: red dot in Fig. 1). The dating analyses showed that the divergence of two South American NT groups (19 MYA) and divergence of *T. ufla* from its sister (9 MYA) (Fig. 3) are both much older than the generally accepted formation age of the Panamanian land bridge. One possible explanation is that the close relatives of this group were once distributed in Central America and went extinct during periods of climate cooling, as occurred in North America. In contrast, although still highly contentious (O'Dea *et al.*, 2016), there are some studies suggesting a Miocene formation of the Isthmus of Panama (Hastings *et al.*, 2013; Montes *et al.*, 2015). A biogeographical study of Neotropical army ants also showed that their ancestors crossed the intermittent Panamanian land bridges between 4 to 7 MYA (Winston, Kronauer & Moreau, in press). These estimated ages would correspond to the divergence between the two NT groups, as well as the split of *T. ufla* from its sister taxa. Morphologically, the South American *T. ufla* is very different from its relatives distributed in Central America (Yoshizawa *et al.*, in press), also suggesting a deep divergence from a Central American ancestor. The occurrence of *Trichadenotecnum* in South America may provide an additional support for the Miocene formation of the Isthmus of Panama.

The *alexanderae* group seems to have a completely different biogeographical history than the NT and NCS clades. Species of this group are distributed in eastern Asia to the

Nearctic (Fig. 1), and they likely dispersed across Beringia (Fig. 4). The divergence date between two *alexanderae* clades was estimated as 0.9 MYA (Fig. 3), but this estimated date is much younger than the assumed formation date of the Bering Strait (3.1–4.1 MYA: Marincovich Jr & Gladenkov, 1999). A biogeographical analysis of blue butterflies also showed that the butterflies migrated to the New World via Beringia multiple times after formation of the Bering Strait (ca. 2.4, 1.1 and 1.0 MYA: Vila *et al.*, 2011): the latter two datings are close to the divergence time of two *alexanderae* clades (Fig. 3). Furthermore, each *alexanderae* clade contains both Japanese and North American populations, which clearly shows the existence of much more recent transcontinental dispersal events (or even ongoing gene flow). A human assisted introduction is also a possibility, especially for explaining the transcontinental occurrence of the genetically homogeneous populations. However, both clades include populations from different continents so that, if this is a result of human assisted introduction, two-way introductions would have to have occurred. Further population genetic study of the *alexanderae* group should clarify these patterns.

In summary, the distributional pattern of *Trichadenotecnum* is consistent with classical explanations for the formation of the Arcto-Tertiary relict biota. Three to four independent dispersal events between the Palearctic and Nearctic regions and two dispersal events crossing the Isthmus of Panama were identified. Most of the dispersal events can be explained by the presence of land bridges, but over-water dispersals were also implicated after the formation of Bering Strait (around 3.1–4.1 MYA) or before formation of the Isthmus of Panama (before ca. 3 MYA). These may indicate trans-oceanic dispersals of the barklice, which is known to occur (e.g. to oceanic islands). However, the existence of land bridges during younger/older ages than generally assumed is also possible. In particular, the age of the Isthmus of Panama has recently been controversial, and *Trichadenotecnum* could be a potential example for the older formation hypotheses.

## **ACKNOWLEDGEMENTS**

We thank the municipal authorities of Santa Catarina Lachatao and Santiago Comaltepec, Oaxaca, particularly to Juan Santiago Hernandez, for their support during the fieldwork. We also thank two anonymous reviewers for their helpful comments. KY thanks Charles Lienhard for providing us a valuable sample from the United Arab Emirates. This study was partly supported by JSPS research grants 24570093 and 15H04409 to KY and NSF grants

DEB-0612938 and DEB-1239788 to KPJ.

## REFERENCES

- Bess EC, Catanach TA, Johnson KP. 2013.** The importance of molecular dating analyses for inferring Hawaiian biogeographical history: a case study with bark lice (Psocidae: Ptycta). *Journal of Biogeography* **41**: 158–167.
- Betz BW. 1983.** Systematics of the *Trichadenotecnum alexandrae* species complex (Psocoptera: Psocidae) based on an investigation of modes of reproduction and morphology. *Canadian Entomologists* **115**: 1329–1354.
- Chaney RW. 1947.** Tertiary centers and migration routes. *Ecological Monographs* **17**: 139–148.
- Denk T, Grimsson F, Zetter R. 2010.** Episodic migration of oaks to Iceland: Evidence for a North Atlantic “land bridge” in the latest Miocene. *American Journal of Botany* **97**: 276–287.
- Denk T, Grimsson F, Zetter R, Simonarson LA. 2011.** Late Cainozoic floras of Iceland. *Topics in Geobiology* **35**: xvi + 1–854.
- Enderlein G. 1911.** Die fossilen Copeognathen und ihre Phylogenie. *Palaeontographica* **58**: 279–360.
- Enderlein G. 1929.** Über die Drüsenhaare der Larve des fossilen *Trichadenotecnum trigonoscenea* (Enderl. 1911). *Zoologischer Anzeiger* **83**: 177–180.
- Engel MS, Perkovsky EE. 2006.** Psocoptera (Insecta. in Eocene Rovno amber (Ukraine). *Vestnik zoologii* **40**: 175–179.
- Hastings AK, Bloch JI, Jaramillo CA, Rincon AF, Macfadden BJ. 2013.** Systematics and biogeography of crocodylians from the Miocene of Panama. *Journal of Vertebrate Paleontology* **33**: 239–263.
- Holt BG, Lessard J-P, Borregaard MK, Fritz SA, Araújo MB, Dimitrov D, Fabre P-H, Graham CH, Graves GR, Jönsson KA, Nogués-Bravo D, Wang Z, Whittaker RJ, Fjeldsa J, Rahbek C. 2013.** An update of Wallace's zoogeographic regions of the world. *Science* **339**: 74–78.
- Lienhard C, Smithers CN. 2002.** *Psocoptera (Insecta): World Catalogue and Bibliography*. Geneva: Muséum d'Histoire Naturelle.

- Lienhard C. 2003–2016.** Additions and corrections (part 1–15) to Lienhard & Smithers, 2002: "Psocoptera (Insecta) –World Catalogue and Bibliography". *Psocid News* **4**: 2–23; **5**: 2–37; **6**: 1–23; **7**: 1–16; **8**: 1–18; **9**: 1–17; **10**: 1–18; **11**: 2–16; **12**: 1–18; **13**: 1–18; **14**: 1–13; **15**: 1–21; **16**: 1–20; **17**: 1–17; **18**: 1–12.
- Maddison WP, Maddison DR. 2016.** Mesquite: a modular system for evolutionary analysis. Version 3.10 <http://mesquiteproject.org>
- Marincovich Jr L, Gladenkov AY. 1999.** Evidence for an early opening of the Bering Strait. *Nature* **397**: 149–151.
- Micheels A, Bruch AA, Uhl D, Utescher T, Mosbrugger V. 2007.** A Late Miocene climate model simulation with ECHAM4/ML and its quantitative validation with terrestrial proxy data. *Palaeogeography, Palaeoclimatology, Palaeoecology* **253**: 251–270.
- Milne RI. 2006.** Northern hemisphere plant disjunctions: A window on Tertiary Land Bridges and climate change? *Annals of Botany* **98**: 465–472.
- Milne Ri, Abbott RJ. 2002.** The origin and evolution of Tertiary relict floras. *Advances in Botanical Research* **38**: 281–314.
- Minh BQ, Nguyen MAT, Haeseler von A. 2013.** Ultrafast Approximation for Phylogenetic Bootstrap. *Molecular Biology and Evolution* **30**: 1188–1195.
- Mockford EL. 1993.** *North American Psocoptera (Insecta)*. Flora & Fauna Handbook No. 10. Gainesville, FL: Sandhill Crane Press.
- Montes C, Cardona A, Jaramillo C, Pardo A, Silva JC, Valencia V, Ayala C, Perez-Angel LC, Rodriguez-Parra LA, Ramirez V, Nino H. 2015.** Middle Miocene closure of the Central American Seaway. *Science*, **348**, 226–229.
- Nguyen L-T, Schmidt HA, Haeseler von A, Minh BQ. 2015.** IQ-TREE: a fast and effective stochastic algorithm for estimating maximum-likelihood phylogenies. *Molecular Biology and Evolution*, **32**, 268–274.
- Nylander JAA. 2004.** *MrModeltest V2*. Program distributed by the author, Evolutionary Biology Centre, Uppsala University.
- O’Dea A, Lessios HA, Coates AG, Eytan RI, Restrepo-Moreno SA, Cione AL, Collins LS, de Queiroz A, Farris DW, Norris RD, Stallard RF, Woodburne MO, Aguilera O, Aubry MP, Berggren WA, Budd AF, Cozzuol MA, Coppard SE, Duque-Caro H, Finnegan S, Gasparini GM, Grossman EL, Johnson KG, Keigwin LD, Knowlton N, Leigh EG, Leonard-Pingel JS, Marko PB, Pyenson ND, Rachello-Dolmen PG,**

- Soibelzon E, Soibelzon L, Todd JA, Vermeij GJ, Jackson JBC. 2016.** Formation of the Isthmus of Panama. *Science Advances* **2**: e1600883.
- Petit RJ, Aguinagalde I, de Beaulieu J-L, Bittkau C, Brewer S, Cheddadi R, Ennos R, Fineschi S, Grivet D, Lascoux M, Mohanty A, Müller-Starck G, Demesure-Musch B, Palmé A, Martín JP, Rendell S, Vendramin GG. 2003.** Glacial refugia: hotspots but not melting pots of genetic diversity. *Science* **300**: 1563–1565.
- Posada D. 2008.** jModelTest: Phylogenetic Model Averaging. *Molecular Biology and Evolution* **25**: 1253–1256.
- Ree RH, Smith SA. 2008.** Maximum Likelihood Inference of Geographic Range Evolution by Dispersal, Local Extinction, and Cladogenesis. *Systematic Biology* **57**: 4–14.
- Roberts DR, Hamann A. 2015.** Glacial refugia and modern genetic diversity of 22 western North American tree species. *Proceedings of the Royal Society B: Biological Sciences* **282**: 20142903.
- Roesler R. 1943.** Über einige Copeognathengenera. *Stettiner Entomologische Zeitung* **104**: 1–14.
- Ronquist F, Huelsenbeck JP. 2003.** MrBayes 3: Bayesian phylogenetic inference under mixed models. *Bioinformatics* **19**: 1572–1574.
- Sanmartín I, Enghoff H, Ronquist F. 2001.** Patterns of animal dispersal, vicariance and diversification in the Holarctic. *Biological Journal of the Linnean Society* **73**: 345–390.
- Swofford D. 2002.** *PAUP\*: phylogenetic analysis using parsimony (\* and other methods*, version 4.0a149. Sunderland, MA: Sinauer Associates.
- Tiffney BH. 1985.** Perspectives on the origin of the floristic similarity between eastern Asia and eastern North America. *Journal of the Arnold Arboretum* **66**: 73–94.
- Vila R, Bell CD, Macniven R, Goldman-Huertas B, Ree RH, Marshall CR, Bálint Z, Johnson K, Benyamini D, Pierce NE. 2011.** Phylogeny and palaeoecology of *Polyommatus* blue butterflies show Beringia was a climate-regulated gateway to the New World. *Proceedings of the Royal Society B: Biological Sciences* **278**: 2737–2744.
- Wagner R, Hoffeins C, Hoffeins HW. 2000.** A fossil nymphomyiid (Diptera) from the Baltic and Bitterfeld amber. *Systematic Entomology* **25**: 115–120.
- Walker MJ, Stockman AK, Marek PE, Bond JE. 2009.** Pleistocene glacial refugia across the Appalachian Mountains and coastal plain in the millipede genus *Narceus*: Evidence from population genetic, phylogeographic and paleoclimatic data. *BMC Evolutionary*

*Biology* **9**: 25.

- Wallace AR. 1876.** *The geographical distribution of animals, with a study of the relations of living and extinct faunas as elucidating the past changes of the earth's surface.* London: Macmillan.
- Wen J. 1999.** Evolution of eastern Asian and eastern North American disjunct distribution in flowering plants. *Annual Review of Ecology and Systematics* **30**: 421–455.
- Winston ME, Kronauer DJC, Moreau CS. In press.** Early and dynamic colonization of Central America drives speciation in Neotropical army ants. *Molecular Ecology* doi: 10.1111/mec.13846
- Wolfe JA. 1994.** An analysis of Neogene climates in Beringia. *Palaeogeography, Palaeoclimatology, Palaeoecology* **108**: 207–216.
- Yang Z. 2007.** PAML 4: phylogenetic analysis by maximum likelihood. *Molecular Biology and Evolution* **24**: 1586–1591.
- Yoshizawa K. 2001.** A systematic revision of Japanese *Trichadenotecnum* Enderlein (Psocodea: 'Psocoptera': Psocidae: Ptyctini), with redefinition and subdivision of the genus. *Invertebrate Taxonomy* **15**: 159–204.
- Yoshizawa K. 2004.** Molecular phylogeny of major lineages of *Trichadenotecnum* and a review of diagnostic morphological characters (Psocoptera: Psocidae). *Systematic Entomology* **29**: 383–394.
- Yoshizawa K, Johnson KP. 2008.** Molecular systematics of the barklouse family Psocidae (Insecta: Psocodea: “Psocoptera”. and implications for morphological and behavioral evolution. *Molecular Phylogenetics and Evolution* **46**: 547–559.
- Yoshizawa K, Johnson KP. 2014.** Phylogeny of the suborder Psocomorpha: congruence and incongruence between morphology and molecular data (Insecta: Psocodea: “Psocoptera”). *Zoological Journal of the Linnean Society* **171**: 716–731.
- Yoshizawa K, Lienhard C. 2015a.** The *alinguum* group, a new species group of the genus *Trichadenotecnum*, with descriptions of two new species from Thailand (Psocodea: 'Psocoptera': Psocidae. *Insecta matsumurana new series* **71**: 179–188.
- Yoshizawa K, Lienhard C. 2015b.** Synonymy of *Cryptopsocus* Li with *Trichadenotecnum* Enderlein (Insecta: Psocodea: “Psocoptera”: Psocidae). and description of three new species. *Zootaxa* **3957**: 480–488.
- Yoshizawa K, García Aldrete AN, Mockford EL. 2008.** Systematics and biogeography of



- the New World species of *Trichadenotecnum* Enderlein (Insecta: Psocodea: "Psocoptera": Psocidae). *Zoological Journal of the Linnean Society* **153**: 651–723.
- Yoshizawa K, Lienhard C, Idris AB. 2014.** *Trichadenotecnum* species from Peninsular Malaysia and Singapore (Insecta: Psocodea: "Psocoptera": Psocidae). *Zootaxa* **3835**: 469–500.
- Yoshizawa K, Yao I, Lienhard C. 2016.** Molecular phylogeny reveals genital convergences and reversals in the barklouse genus *Trichadenotecnum* (Insecta: Psocodea: "Psocoptera": Psocidae). *Molecular Phylogenetics and Evolution* **94**: 358–364.
- Yoshizawa K, Souza-Silva M, Ferreira RL. In press.** Disjunct occurrence of *Trichadenotecnum s. str.* in southeastern Brazil (Psocodea: "Psocoptera": Psocidae), with description of a new species. *Neotropical Entomology* doi 10.1007.s13744-016-0449-z
- Yu Y, Harris AJ, Blair C, He X. 2015.** RASP (Reconstruct Ancestral State in Phylogenies): A tool for historical biogeography. *Molecular Phylogenetics and Evolution* **87**: 46–49.
- Zachos J, Pagani M, Sloan L, Thomas E, Billups K. 2001.** Trends, rhythms, and aberrations in global climate 65 Ma to present. *Science* **292**: 686–693.

## Figure captions

**Figure 1.** Map showing the distributional range of three clades of New World *Trichadenotecnum* (cf. Betz, 1983; Mockford, 1993; Yoshizawa, 2001; Yoshizawa *et al.*, 2008, in press). All other *Trichadenotecnum* species are distributed in the Old World. Two possible dispersal gateways, Beringia and North Atlantic Landbridge (NALB), connecting the Palearctic and Nearctic Regions are also indicated.

**Figure 2.** Maximum likelihood tree estimated by PAUP\* with TBR branch swapping using the tree estimated by MrBayes as the starting tree. Clades composed of New World species are highlighted by squares (color corresponds to Fig. 1). A and B indicate the calibration points (see text for detail). Node support values are indicated by asterisks as follow: \*\*\* BS $\geq$ 95 and PP=100, \*\* BS $\geq$ 80 and PP $>$ 95, \* PP $\geq$ 95. Actual support values for some key nodes are mentioned in the text.

**Figure 3.** Chronogram of *Trichadenotecnum* estimated by Bayesian MCMC method. Key divergence events and their ages mentioned in the text are highlighted. Clades composed of New World species are highlighted by squares (color corresponds to Fig. 1).

**Figure 4.** Ancestral area reconstruction of *Trichadenotecnum* based on the DEC model. Permitted dispersal patterns preset in the DEC analysis are indicated by arrows on the map. Pie charts on the nodes indicate likelihood of the estimated ancestral area. See Appendix S3 for detailed statistics of the estimated ancestral area. Clades composed of New World species are highlighted by squares (color corresponds to Fig. 1). A. Afrotropical; B. Western Palearctic; C. Eastern Palearctic; D. Oriental; E. North America; F. Central America; G. South America.

**Figure 5.** Ancestral area reconstruction of the *alexanderae* group based on the likelihood Stochastic Character model. Pie charts on the nodes indicate likelihood of the estimated ancestral area.

**Table 1.** Samples newly included in the present analyses. See Yoshizawa & Johnson (2008)

and Yoshizawa *et al.* (2016) for the other samples. – indicates missing character.

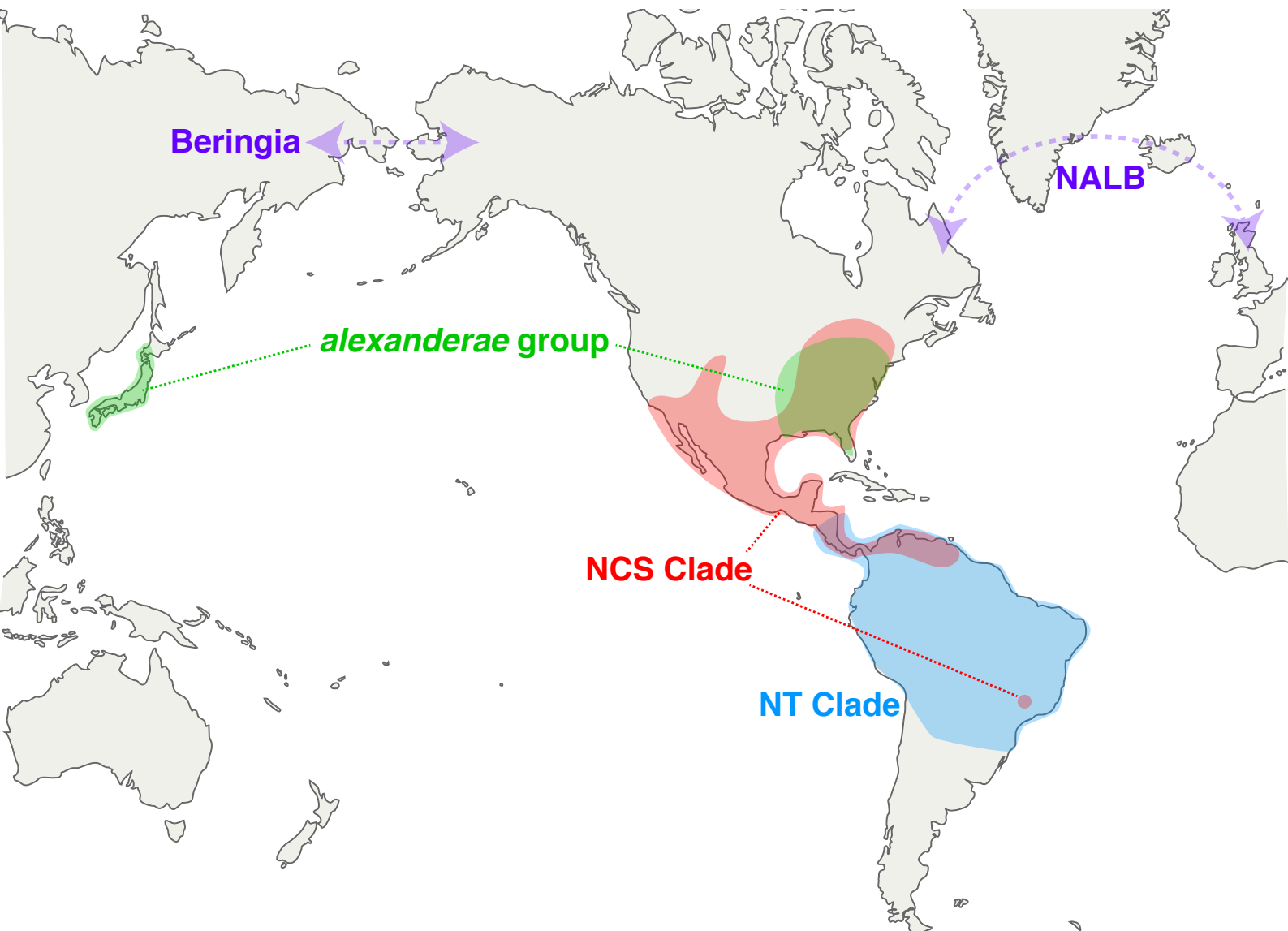
## **SUPPORTING INFORMATION**

**Appendix S1.** Nexus formatted molecular data matrix (five genes) used in this study.

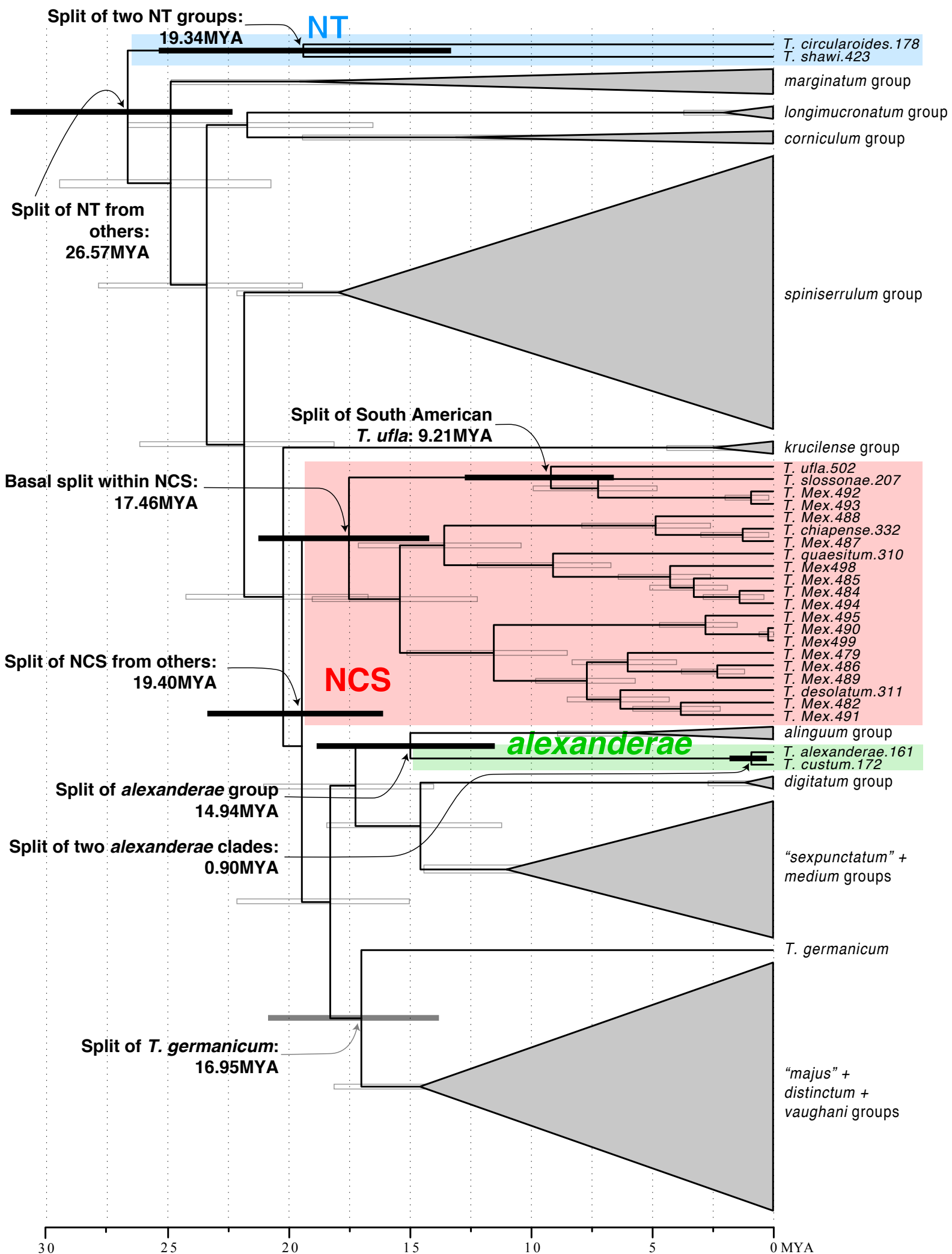
**Appendix S2.** Nexus formatted molecular data matrix (*COI* for the *alexanderae* group) used in this study.

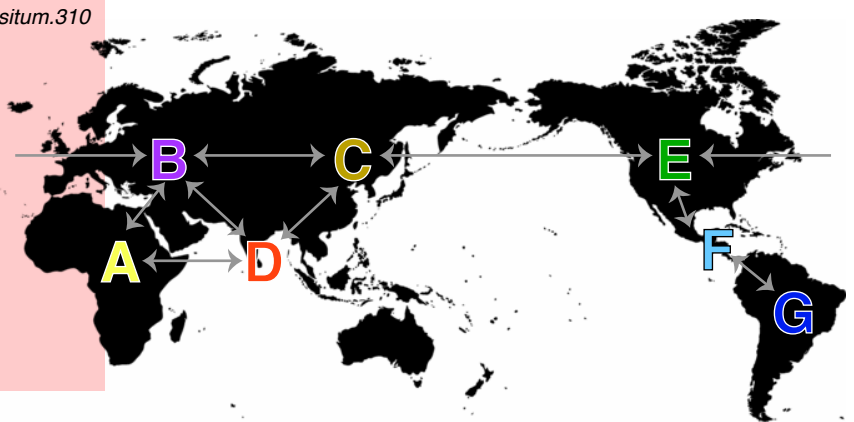
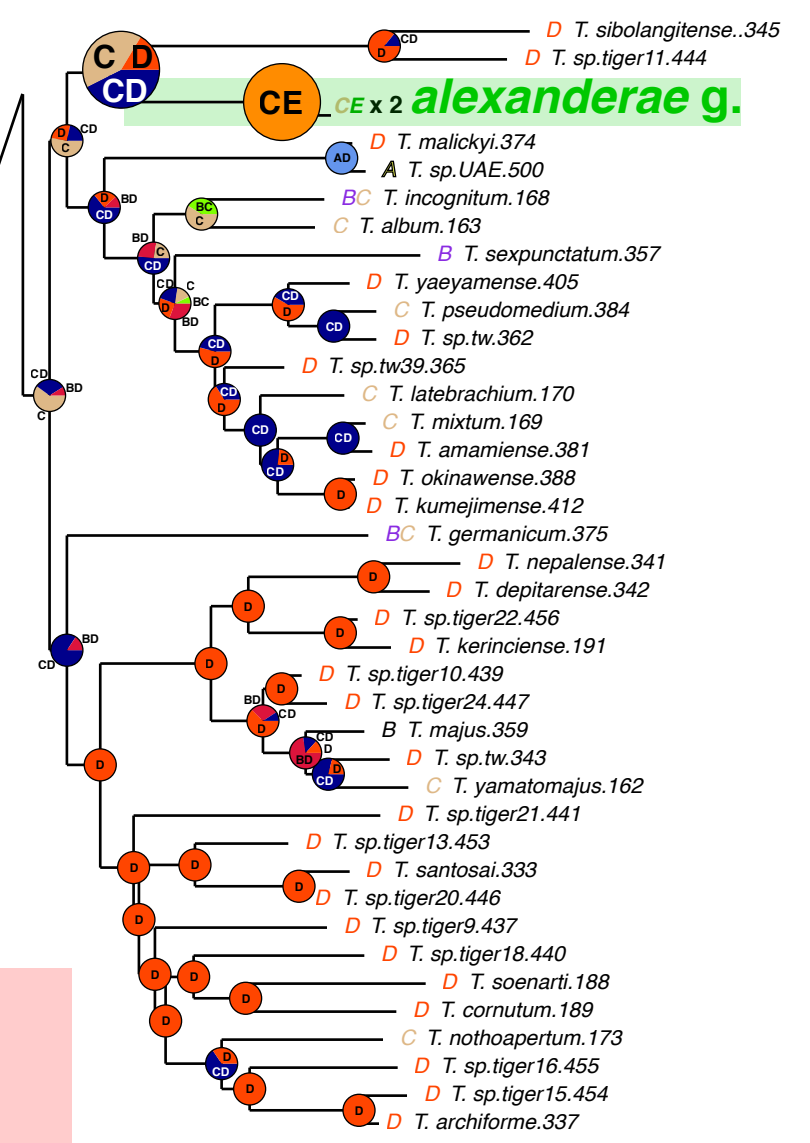
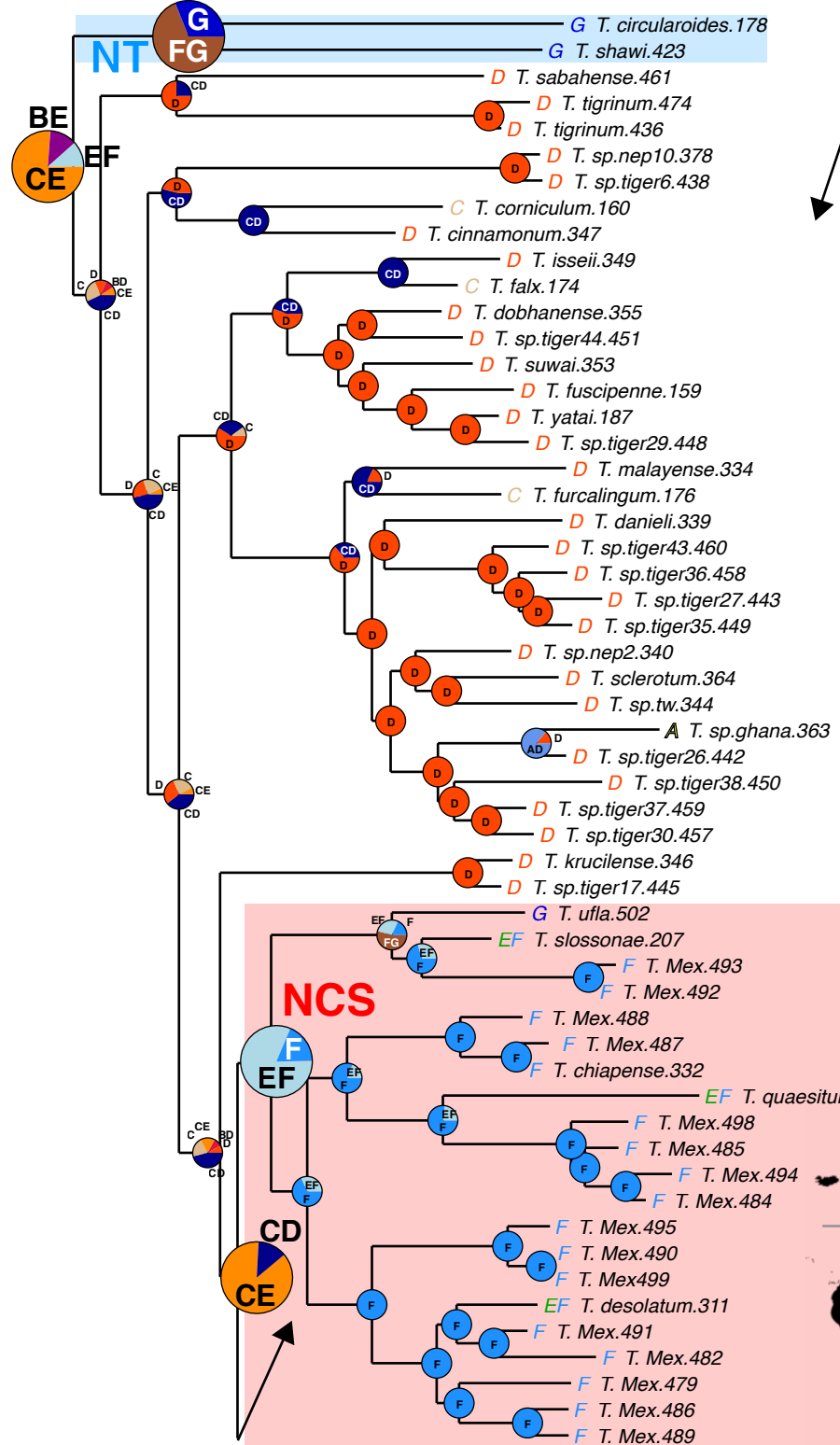
**Appendix S3.** Result of the Lagrange analysis based on the ML tree.

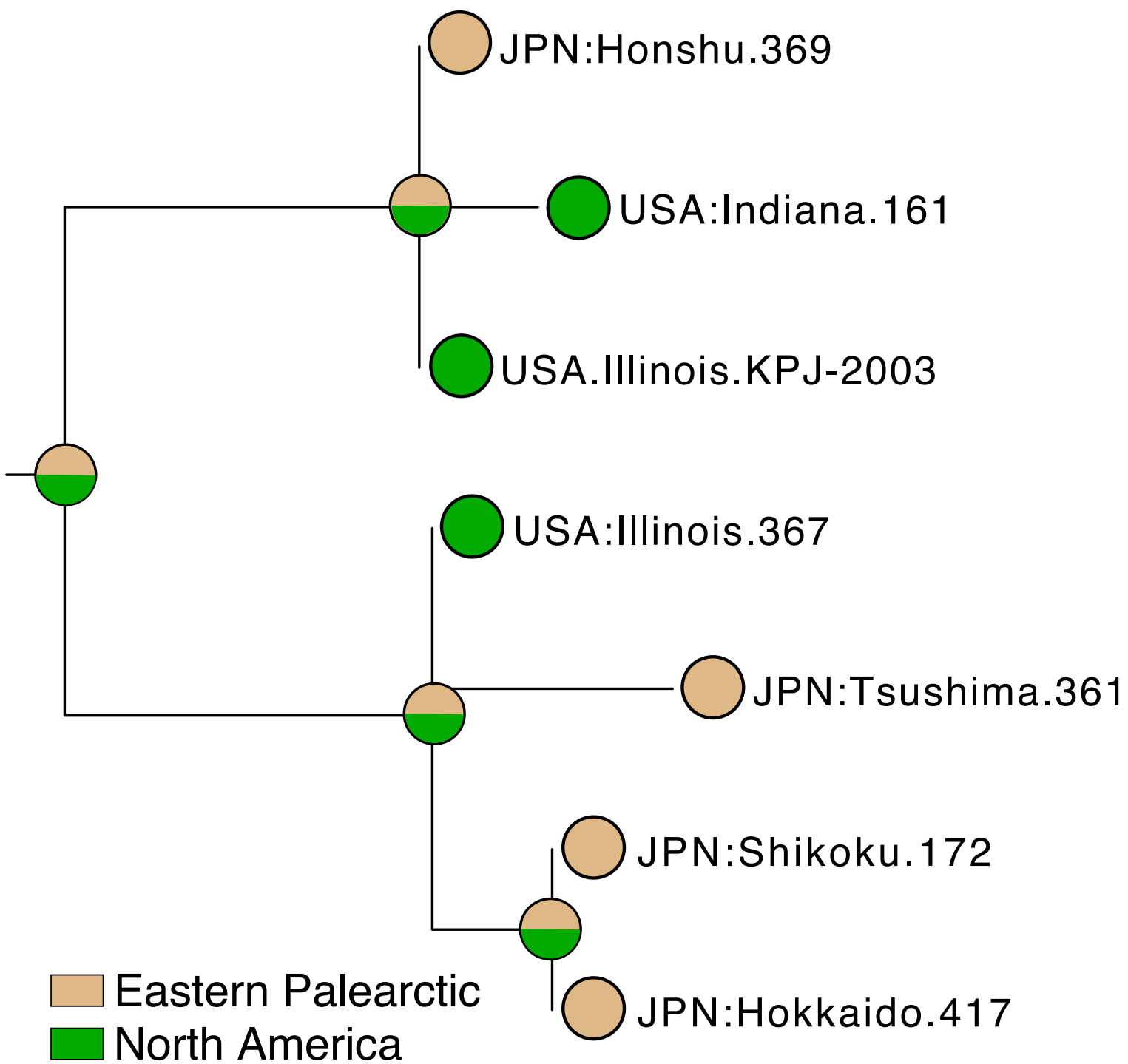
**Appendix S4.** Result of the Lagrange analysis based on the the alternative tree (monophyly of NCS + *kruciliense* group constrained).













Sample name	Voucher ID	Locality	16S	12S	COI	18S	H3
<i>Trichadenotecnum shawi</i>	KY423	Brazil: Goias	–	LC208961	LC209000	–	LC209060
<i>Trichadenotecnum desolatum</i>	KY311	USA: Arizona	EF662137	EF662263	EF662099	EF662297	EF662182
<i>Trichadenotecnum quaesitum</i>	KY310	USA: Arizona	EF662262	EF662136	EF662098	EF662296	EF662181
<i>Trichadenotecnum slossonae</i>	KY207	USA: Illinois	LC208995	LC208975	LC209015	LC209036	LC209068
<i>Trichadenotecnum chiapense</i>	KY332	Belize	LC208996	LC208976	–	LC209037	–
<i>Trichadenotecnum sp.Mex.479</i>	KY479	Mexico: Hidalgo	LC208979	LC208962	LC209001	LC209022	–
<i>Trichadenotecnum sp.Mex.481</i>	KY481	Mexico: Oaxaca	LC208980	LC208963	LC209002	LC209023	–
<i>Trichadenotecnum sp.Mex.482</i>	KY482	Mexico: Queretaro	LC208981	LC208964	LC209003	LC209024	–
<i>Trichadenotecnum sp.Mex.484</i>	KY484	Mexico: Veracruz	LC208983	–	–	LC209025	–
<i>Trichadenotecnum sp.Mex.485</i>	KY485	Mexico: Oaxaca	LC208984	LC208965	LC209004	LC209026	–
<i>Trichadenotecnum sp.Mex.486</i>	KY486	Mexico: Oaxaca	LC208985	LC208966	LC209005	LC209027	LC209061
<i>Trichadenotecnum sp.Mex.487</i>	KY487	Mexico: Oaxaca	LC208986	LC208967	LC209006	LC209028	–
<i>Trichadenotecnum sp.Mex.488</i>	KY488	Mexico: Chiapas	LC208987	LC208968	LC209007	LC209029	–
<i>Trichadenotecnum sp.Mex.489</i>	KY489	Mexico: Hidalgo	LC208988	LC208969	LC209008	LC209030	LC209062
<i>Trichadenotecnum sp.Mex.490</i>	KY490	Mexico: Oaxaca	LC208989	LC208970	LC209009	LC209031	LC209063
<i>Trichadenotecnum sp.Mex.491</i>	KY491	Mexico: Queretaro	LC208990	LC208971	LC209010	LC209032	LC209064
<i>Trichadenotecnum sp.Mex.492</i>	KY492	Mexico: Queretaro	LC208991	LC208972	LC209011	LC209033	–
<i>Trichadenotecnum sp.Mex.493</i>	KY493	Mexico: Hidalgo	LC208992	–	LC209012	–	LC209065
<i>Trichadenotecnum sp.Mex.494</i>	KY494	Mexico: Hidalgo	LC208993	LC208973	LC209013	LC209034	LC209066
<i>Trichadenotecnum sp.Mex.495</i>	KY495	Mexico: Oaxaca	LC208994	LC208974	LC209014	LC209035	LC209067
<i>Trichadenotecnum sp.Mex.498</i>	KY498	Mexico: Oaxaca	LC208997	LC208977	LC209016	LC209038	–
<i>Trichadenotecnum sp.Mex.499</i>	KY499	Mexico: Oaxaca	LC208998	LC208978	LC209017	LC209039	LC209069
<i>Trichadenotecnum ufla.502</i>	KY502	Brazil: Minas Gerais	LC185091	LC185092	LC185093	LC185094	LC185095
<i>Trichadenotecnum sp.UAE.500</i>	KY500	UAE	LC208999	–	–	LC209059	LC209089
<i>Ptycta pikeloi</i>	Pt021.MO.10.13.2008.2	Hawaii: Molokai	KF499163	KF651849	KF651730	LC209040	LC209070
<i>Ptycta molokaiensis</i>	Pt024.MO.10.13.2008.2	Hawaii: Molokai	KF499165	KF651851	KF651732	LC209041	LC209071
<i>Ptycta apicantha</i>	Pt032.HI.10.06.2008.02	Hawaii: Hawaii	KF499172	KF651858	KF651739	LC209042	LC209072
<i>Ptycta maculifrons</i>	Pt036.HI.10.06.2008.06	Hawaii: Hawaii	KF499176	KF651862	KF651743	LC209043	LC209073
<i>Ptycta hardyi</i>	Pt037.HI.10.06.2008.07	Hawaii: Hawaii	KF499177	KF651863	KF651744	LC209044	LC209074
<i>Ptycta simulator kilauea</i>	Pt039.HI.10.06.2008.09	Hawaii: Hawaii	KF499179	KF651865	KF651746	LC209045	LC209075
<i>Ptycta maculifrons</i>	Pt040.HI.10.06.2008.10	Hawaii: Hawaii	KF499180	KF651866	KF651747	LC209046	LC209076
<i>Ptycta sp.Pt045</i>	Pt045.HI.10.06.2008.15	Hawaii: Hawaii	KF499185	KF651871	KF651752	LC209047	LC209077
<i>Ptycta diadela</i>	Pt026.OH.01.06.2009.0	Hawaii: Oahu	KF499167	KF651853	KF651734	LC209048	LC209078
<i>Ptycta sp.Pt029</i>	Pt029.OH.01.06.2009.0	Hawaii: Oahu	KF499169	KF651855	KF651736	LC209049	LC209079
<i>Ptycta placophora</i>	Pt030.OH.01.06.2009.0	Hawaii: Oahu	KF499170	KF651856	KF651737	LC209050	LC209080
<i>Ptycta maculifrons</i>	Pt052.HI.01.06.2009.08	Hawaii: Hawaii	KF499191	KF651877	KF651758	LC209051	LC209081
<i>Ptycta sp.Pt055</i>	Pt055.HI.01.06.2009.09	Hawaii: Hawaii	KF499193	KF651879	KF651760	LC209052	LC209082
<i>Ptycta monticola</i>	Pt075.KA.03.31.2009.03	Hawaii: Kauai	KF499206	KF651892	KF651773	LC209053	LC209083
<i>Ptycta telma</i>	Pt076.KA.03.31.2009.04	Hawaii: Kauai	KF499207	KF651893	KF651774	LC209054	LC209084
<i>Ptycta palikea</i>	Pt078.OH.03.31.2009.0	Hawaii: Oahu	KF499209	KF651895	KF651776	LC209055	LC209085
<i>Ptycta apicantha</i>	Pt043.HI.03.31.2009.13	Hawaii: Hawaii	KF499182	KF651868	KF651749	LC209056	LC209086
<i>Ptycta sp.Pt060</i>	Pt060.MA.03.31.2009.1	Hawaii: Maui	KF499196	KF651882	KF651763	LC209057	LC209087
<i>Ptycta diastema</i>	Pt012.KA.03.31.2009.11	Hawaii: Kauai	KF499159	KF651845	KF651726	LC209058	LC209088
<i>T. alexandrae complex</i>	KY172	Japan: Shikoku	–	–	AY374558	–	–
<i>T. alexandrae complex</i>	KY361	Japan: Tsushima	–	–	LC209020	–	–
<i>T. alexandrae complex</i>	KY369	Japan: Honshu	–	–	LC209018	–	–
<i>T. alexandrae complex</i>	KY417	Japan: Hokkaido	–	–	LC209021	–	–
<i>T. alexandrae complex</i>	KY161	USA: Indiana	–	–	AY374564	–	–
<i>T. alexandrae complex</i>	KY367	USA: Illinois	–	–	LC209019	–	–
<i>T. alexandrae complex</i>	KPJ-2003	USA: Illinois	–	–	AY275287	–	–